ELSEVIER

International Journal of Heat and Fluid Flow 23 (2002) 615–626

International Journal of HEAT AND FLUID FLOW

www.elsevier.com/locate/ijhff

Turbulence modification in a homogeneous turbulent shear flow laden with small heavy particles

Mitsuru Tanaka *, Yasushi Maeda, Yoshimichi Hagiwara

Department of Mechanical and System Engineering, Kyoto Institute of Technology, 606-8585 Kyoto, Japan

Abstract

Numerical simulations have been conducted for a homogeneous turbulent shear flow laden with small heavy particles in order to investigate the modification of turbulence structures in shear flows due to particles. The effects on the turbulence modification of gravitational settling of particles in the sheared direction are examined for the particles whose response times are comparable to the Kolmogorov time-scale of turbulence. It is found that the growth rate of turbulence energy of the carrier fluid, which is reduced by the particles in zero gravity, is increased by the effect of weak gravity through the enhancement of Reynolds shear stress, but decreased by the effect of strong gravity through the increase in drag dissipation. It is shown in finite gravity that particle clusters are generated due to the accumulation of particles in two types of regions; downward flows sandwiched between counter rotating quasi-streamwise vortex tubes and regions just beneath the vortex layers with negative spanwise vorticity. The particle clusters between the pair vortex tubes intensify the downward flows between them to enhance the Reynolds shear stress, while the particle clusters beneath the vortex layers enhance the drag dissipation of fluid turbulence energy in the streamwise direction. The downward flows induced by particle clusters activate the tilting of the spanwise vorticity toward the vertical direction. © 2002 Elsevier Science Inc. All rights reserved.

Keywords: Small heavy particles; Gravity; Numerical simulation; Uniform shear; Turbulence; Vortical structures; Particle clusters

1. Introduction

Turbulent gas flows with heavy particles have attracted our attention because they are encountered in nature and industries. Many studies have been carried out to understand the flow characteristics, and the interaction between particles and gas flow turbulence. Experimental data indicate that addition of small particles attenuates turbulence, while that of large particles augments turbulence of the gas flows in a horizontal pipe (Tsuji and Morikawa, 1982), a vertical pipe (Tsuji et al., 1984), a vertical boundary layer (Rogers and Eaton, 1991) and a vertical channel (Kulick et al., 1994). However, these wall-bounded flows contain both shear-dominant, and inhomogeneous turbulence in near-wall regions and nearly homogeneous turbulence in the core regions. Therefore, the mechanism of the interaction has not yet been fully understood from these data.

Some details of the interaction in homogeneous isotropic turbulent gas flow have been clarified by the use of numerical simulations. Squires and Eaton (1990) found in their numerical simulation of forced homogeneous isotropic turbulence that the particles reduces the kinetic energy of the carrier fluid flow. Elghobashi and Truesdell (1993) showed that the particles in gravity increases the kinetic energy of the carrier fluid flow as a result of an inverse cascade of turbulence energy.

The clustering of the particles due to the interaction in isotropic turbulent gas flow has been also discussed from numerical or experimental results. Squires and Eaton (1990, 1991) found the tendency of the particles to accumulate in low-vorticity or high-strain regions. Wang and Maxey (1993) have shown that the particles in gravity tend to accumulate in downward flows, which increases the mean settling velocity of the particles. Recent experimental (Aliseda et al., 2002) and numerical (Tanaka et al., 2000) studies indicate that the particle accumulation or clustering causes the significant increase in the particle settling velocity due to the effect of the two-way coupling between the particles and the

* Corresponding author.
E-mail addresses: mtanaka@ipc.kit.ac.jp (M. Tanaka), yoshi@ipc.kit.ac.jp (Y. Hagiwara).

0142-727X/02/$ - see front matter © 2002 Elsevier Science Inc. All rights reserved.
PII: S0142-727X(02)00157-1

Nomenclature

c	normalization constant for initial energy spectrum
$\overline{C}$, C	mean and local volume fractions of particles
E	turbulence kinetic energy of carrier fluid
$E(k)$	energy spectrum
F	source/sink of E due to phase interaction
F_{ij}	source/sink of $\langle u_i' u_j' \rangle$ due to phase interaction
f_i	reaction force exerted by particles on fluid
f_i'	fluctuating part of f_i
g	gravitational acceleration
k_0	wavenumber at which the initial energy spectrum takes its maximum
$k_{\max}$	maximum wavenumber, $N/2$
N	number of grid points in each direction
p, p'	total and fluctuating pressures
R_λ	Taylor-microscale Reynolds number, $R_\lambda = \langle \boldsymbol{u}'^2 \rangle / \nu \sqrt{\langle \boldsymbol{\omega}'^2 \rangle}$
S^*	shear rate parameter, $S^* = \gamma \langle \boldsymbol{u}'^2 \rangle / \nu \langle \boldsymbol{\omega}'^2 \rangle$
u_i, u_i'	fluid velocity and its fluctuating component
v_i, v_i'	particle velocity and its deviation from the mean shear
V_S	still-fluid terminal velocity of particle
w_{ij}	vorticity anisotropy tensor, $w_{ij} = \langle \omega_i' \omega_j' \rangle / \langle \omega_k' \omega_k' \rangle - (1/3)\delta_{ij}$
x_i	coordinate
y_i	position of particle
α, β	orientation angles of vorticity vector
δ_{ij}	Kronecker delta
ϵ	dissipation rate of fluid kinetic energy
γ	shear rate
η	Kolmogorov length-scale of turbulence
ν	fluid viscosity
ρ_f, ρ_p	fluid and particle densities
τ_K	Kolmogorov time-scale of turbulence
τ_p	particle response time
ω_i, ω_i'	total and fluctuating vorticity components
$\langle\,\rangle$	spatial average
$\langle\,\rangle_p$	ensemble average over particles

Superscript

$+$	Normalization by Kolmogorov scales

fluid flow. However, the relationship between particle clustering and turbulence modulation has not yet been well understood.

On the other hand, some details of the interaction in homogeneous turbulent shear flows have been discussed recently by the use of numerical simulations (Mashayek, 1998; Ahmed and Elghobashi, 2000). Mashayek (1998) found that the presence of particles in zero gravity decreases the turbulence energy of the carrier fluid flow and increases the anisotropy of the velocity field due to the two-way coupling effect. Ahmed and Elghobashi (2000) examined the modification of turbulence for particles in zero and finite gravities to find that the effect of gravity enhances the growth of turbulence. They also investigated the modification of the vorticity dynamics by particles. However, the modification of vortical structures and their dynamics, which may control the dynamics of turbulence, has not been examined in detail. In particular, no attentions have been focused on the shear layer (vortex layer), which is one of the major vortical structures in homogeneous turbulent shear flows (Kida and Tanaka, 1994).

In the present study, the accumulation of particles and turbulence modification in a homogeneous turbulent shear flow are examined by the use of numerical simulation. We particularly focus on the interaction between vortical structures and particle clusters, which is expected to control the development of turbulence.

2. Formulation

2.1. Fluid and particle motions

We consider the motions of small heavy spherical particles in homogeneous turbulence subjected to the mean flow in the x_1 direction that is uniformly sheared in the x_2 direction, $\bar{\boldsymbol{u}} = (\gamma x_2, 0, 0)$, where γ is the shear rate (see Fig. 1). The particle is assumed to be small enough,

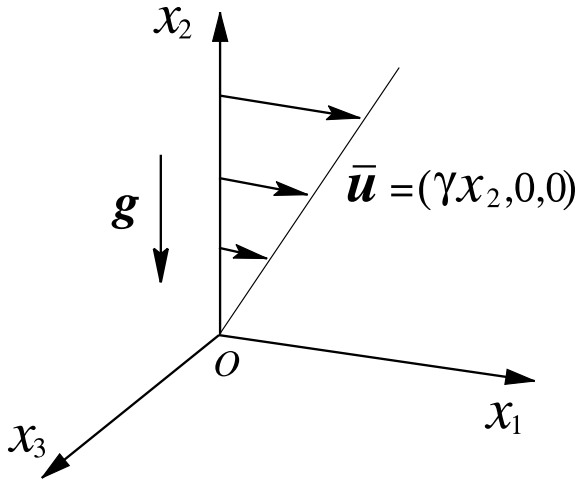

Fig. 1. Configuration.

compared to the Kolmogorov length-scale η of the turbulence. Since we consider the particles of high density ratio, only Stokes drag and gravitational forces are assumed to act on the particles (Maxey and Riley, 1983). In this study, we consider the gravity in the negative x_2 direction. The particulate phase is assumed to be dilute enough that the effects of inter-particle collisions are neglected though the two-way interaction between two phases is taken into account.

The motions of the carrier fluid are described by

$$\frac{\partial u_i}{\partial t} + u_k \frac{\partial u_i}{\partial x_k} = -\frac{1}{\rho_f}\frac{\partial p}{\partial x_i} - g\delta_{i2} + \nu\nabla^2 u_i + \frac{1}{\rho_f} f_i \tag{1}$$

with the solenoidal condition $\partial u_j/\partial x_j = 0$, where u_i, ρ_f, p, and ν are the velocity, density, pressure, and kinematic viscosity of the fluid, respectively. g denotes the gravitational acceleration. f_i represents a body force which is the sum of the reaction forces exerted by the particles on the fluid. Let us decompose the velocity into the mean shear and the fluctuation,

$$u_i = \gamma x_2 \delta_{i1} + u_i'. \tag{2}$$

Substituting Eq. (2) for Eq. (1), we obtain the equation for the fluctuating velocity as

$$\frac{\partial u_i'}{\partial t} + \gamma x_2 \frac{\partial u_i'}{\partial x_1} + u_k' \frac{\partial u_i'}{\partial x_k} = -\gamma u_2' \delta_{i1} - \frac{1}{\rho_f}\frac{\partial p'}{\partial x_i} + \nu\nabla^2 u_i' + \frac{1}{\rho_f} f_i', \tag{3}$$

where $p' = p - \langle p\rangle$ and $f_i' = f_i - \langle f_i\rangle$. $\langle\,\rangle$ denotes the spatial average. Here, the spatial average of f_i and the term, $-g\delta_{i2}$, in Eq. (1) are assumed to be balanced by the mean pressure gradient, that is, $-(1/\rho_f)\partial\langle p\rangle/\partial x_i - g\delta_{i2} + \langle f_i\rangle/\rho_f = 0$. Ahmed and Elghobashi (2000) considered this type of pressure balance only in the vertical direction though $\langle f_1\rangle$ is generally non-zero in a shear flow under gravity, as is indicated by Eq. (6). We have carried out a computation with the same pressure balance as in Ahmed and Elghobashi (2000) to confirm that the effects of the difference in the pressure balance are slight within the range of parameters considered in this study.

The particulate phase is tracked in the Lagrangian frame. The motion of the spherical particle with diameter, d_p, is described by

$$\frac{dv_i}{dt} = \frac{1}{\tau_p}(u_i(\boldsymbol{y}) - v_i - V_S\delta_{i2}), \quad \frac{dy_i}{dt} = v_i, \tag{4}$$

where y_i and v_i denote the position and the velocity of the particle, respectively, and $u_i(\boldsymbol{y})$ represents the velocity of the surrounding fluid. τ_p is the particle response time, which is given by $\rho_p d_p^2/18\rho_f\nu$ for Stokes flow, where ρ_p is the density of the solid particle. $V_S = \tau_p g$ is the still-fluid terminal velocity of the particle due to the gravity. Decomposing the particle velocity as in Eq. (2),

$$v_i = \gamma x_2 \delta_{i1} + v_i', \tag{5}$$

we obtain the evolution equation for v_i' as

$$\frac{dv_i'}{dt} = \frac{d}{dt}(v_i - \gamma x_2\delta_{i1}) = -\gamma v_2'\delta_{i1} + \frac{1}{\tau_p}\left(u_i'(\boldsymbol{y}) - v_i' - V_S\delta_{i2}\right). \tag{6}$$

Eq. (6) indicates that in a laminar simple shear flow the particle moves faster than the mean shear at the particle position by $v_1' = -\gamma\tau_p v_2' = \gamma\tau_p^2 g > 0$ for $t \gg \tau_p$. This means that particles in the simple shear flow drag the fluid not only in the negative x_2 (gravitational) direction but also in the positive x_1 direction. Since, in the present study, the particles are distributed homogeneously due to the periodicity of the computational domain (Section 2.3), the carrier fluid turbulence, which would be modified by the presence of the particles, remains homogeneous in space.

2.2. Turbulence energy

The time development of turbulence kinetic energy of the carrier fluid, $E = (1/2)\langle u_k' u_k'\rangle$, is described by

$$\frac{dE}{dt} = -\gamma\langle u_1' u_2'\rangle - \epsilon + F. \tag{7}$$

The first and second terms on the right-hand side of Eq. (7) represent the rate of turbulence energy production and the rate of turbulence energy dissipation, respectively. F denotes the energy transfer to the fluid phase due to the direct interaction with the particulate phase through Stokes drag force;

$$\begin{aligned} F &= (1/2)F_{kk}, \\ F_{ij} &= \frac{1}{\rho_f}\left\langle f_i u_j' + f_j u_i'\right\rangle \\ &= \frac{\rho_p}{\rho_f}\frac{\overline{C}}{\tau_p}\left\langle u_i'(\boldsymbol{y})\left(u_j'(\boldsymbol{y}) - v_j'\right) + u_j'(\boldsymbol{y})\left(u_i'(\boldsymbol{y}) - v_i'\right)\right\rangle_p, \end{aligned} \tag{8}$$

where $\overline{C}$ represents the mean volume fraction of particles, and $\langle\,\rangle_p$ denotes the ensemble average over particles. The last term in Eq. (8) was obtained by using the homogeneity of the particle distribution.

2.3. Numerical method

Eq. (3) with the solenoidal condition $(\partial u_j'/\partial x_j = 0)$ was solved on 128^3 grid points in a rectangular box of sides $4\pi \times 2\pi \times 2\pi$, by using the Fourier spectral/Runge–Kutta–Gill scheme. The initial velocity field was given by the Fourier coefficients with a specified energy spectrum,

$$E(k) = ck^4 \exp\left(-2k^2/k_0^2\right), \tag{9}$$

and with a random phase. Here, c is a normalization constant and k_0 is a wavenumber at which the energy spectrum takes the maximum. Homogeneous turbulent shear flows are characterized by the two parameters; the (Taylor-microscale) Reynolds number $R_\lambda(t) =$

$\langle \boldsymbol{u}'^2 \rangle / v\sqrt{\langle \boldsymbol{\omega}'^2 \rangle}$ and the shear rate parameter $S^*(t) = \gamma \langle \boldsymbol{u}'^2 \rangle / v \langle \boldsymbol{\omega}'^2 \rangle$, where $\boldsymbol{\omega}' = \nabla \times \boldsymbol{u}'$ denotes the fluctuating vorticity. As in Kida and Tanaka (1992, 1994), the initial values of these two parameters were set as $R_\lambda(0) = 16$ and $S^*(0) = 16$, whereas a smaller value of k_0 was employed in this simulation to obtain higher small-scale resolution.

We have performed computations for 12 types of particles with different values of inertia and settling velocity, $\tau_p^+ \equiv \tau_p/\tau_K = 0.5$, 1.0, 2.0 and $V_S^+ \equiv \tau_K V_S/\eta = 0$, 1, 2, 4, where τ_K is the Kolmogorov time-scale of the turbulence. We introduced 2^{21} (=2 097 152) particles randomly throughout the computational domain at the non-dimensional time of $\gamma t = 4$ where the turbulence had attained the quasi-equilibrium state (Kida and Tanaka, 1992). Each computation was conducted until $\gamma t = 12$. Since the Kolmogorov scales, τ_K and η, decrease gradually with time, their values at the middle time ($\gamma t = 8$) were adopted as the representatives of the scales through the period of the computation.

The particle volume fraction was $\overline{C} = 8.24 \times 10^{-5}$. Recently, Yamamoto et al. (2001) have found in their numerical simulations of gas–solid turbulent flows in a vertical channel that inter-particle collisions play an important role in the interaction between particle motion and gas turbulence even for a solid volume fraction of $O(10^{-4})$. We have checked that the particle mean free times are much ($O(10^2)$ times) longer than the particle response time. Therefore, the effects of inter-particle collisions may be neglected in our simulation. The parameters employed in this simulation are summarized in Table 1.

The initial particle velocity was set to be the same as the surrounding fluid velocity. Third-order Lagrange interpolation was used both for the evaluation of fluid velocity at the particle position from its neighboring grid points and for the distribution to the grid points of the reaction force exerted by the particle on the fluid (Sundaram and Collins, 1996). $k_{max}\eta$ was 1.80 at $\gamma t = 4$, where $k_{max} = N/2$ ($N = 128$) is the maximum wavenumber. We integrated Eq. (4) using the Runge–Kutta–Gill scheme. In zero gravity, the particle Reynolds number remained less than unity throughout the computation for more than 99% of particles, though, in the case of $V_S^+ = 4$, it exceeded unity for about 10% of particles at the end of the computation ($\gamma t = 12$). In this study, we focus on the case of $\tau_p^+ = 1$, and the effects of gravity are examined by changing the value of V_S^+ as $V_S^+ = 0$, 2, 4.

Table 1
Parameters for numerical simulation

c	k_0	γ	ν	ρ_p/ρ_f	d_p	τ_p	V_S	$\overline{C}$	d_p/η	τ_p/τ_K	$V_S\tau_K/\eta$	$V_S/\sqrt{\langle \boldsymbol{u}'^2 \rangle/3}$
6.91×10^{-6}	6.50	1.0	1.18×10^{-3}	1000	3.34×10^{-3}	0.525	0.0474	8.24×10^{-5}	0.134	1.0	1.0	0.341

Particle parameters are shown for the case of $\tau_p^+ = 1$ and $V_S^+ = 1$. Normalization was done by the use of turbulence quantities in the single-phase flow at $\gamma t = 8$. For the cases of $V_S^+ = 0$, 2 and 4, V_S is simply multiplied by 0, 2 and 4, respectively. For the cases of $\tau_p^+ = 0.5$ and 2.0, τ_p is simply multiplied by 0.5 and 2.0, but d_p is multiplied by $\sqrt{0.5}$ and $\sqrt{2.0}$, respectively.

3. Results

3.1. Turbulence energy

Fig. 2 shows the time development of turbulence kinetic energy of the carrier fluid which is normalized by

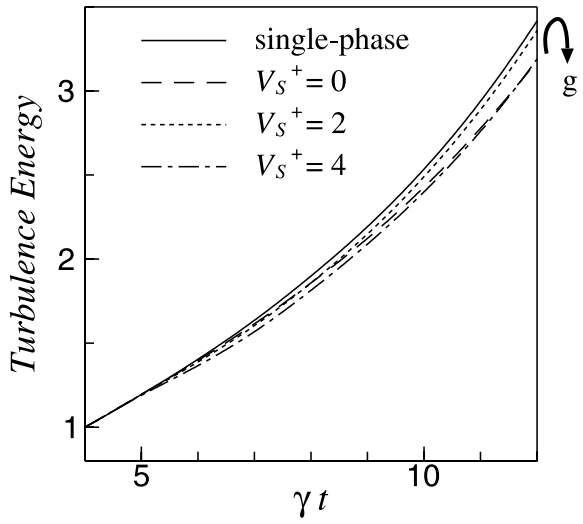

Fig. 2. Time development of turbulence kinetic energy of the carrier fluid: (—) single-phase, (- - -) $V_S^+ = 0$, (···) $V_S^+ = 2$, (–·–) $V_S^+ = 4$.

the value at the time of particle injection ($\gamma t = 4$). As reported before (Kida and Tanaka, 1992), the turbulence energy in the single-phase flow increases exponentially in time. It is seen that the growth of turbulence energy is suppressed by the injection of the particles in zero gravity as was shown in Mashayek (1998). For the case of $V_S^+ = 2$, except at initial times, the particles in the gravity increase the turbulence energy compared to the case of zero gravity. This is in agreement with the result in Ahmed and Elghobashi (2000). However, a further increase of the gravity again attenuates the growth of turbulence ($V_S^+ = 4$).

In order to understand the mechanisms of the turbulence modification, we consider the budget for the turbulence kinetic energy (Eq. (7)). Fig. 3 shows the time development of the non-dimensional growth rate of energy, $(1/E)\mathrm{d}E/\mathrm{d}(\gamma t)$, which obeys

$$\frac{1}{\gamma E}\frac{\mathrm{d}E}{\mathrm{d}t} = -\frac{\langle u_1' u_2'\rangle}{E} - \frac{\epsilon}{\gamma E} + \frac{F}{\gamma E}. \tag{10}$$

The production (first), the dissipation (second), and the phase-interaction (third) terms in the right-hand side of Eq. (10) are also plotted in Fig. 3. The attenuation of turbulence in zero gravity is triggered mainly by the decrease in the production of turbulence energy, though the phase-interaction term also contributes to the decrease of the energy particularly at later times when the effective particle inertia, $\tau_\mathrm{p}/\tau_\mathrm{K}$, becomes larger. It is found that the presence of particles reduces the energy production, $-\gamma\langle u_1' u_2'\rangle$, directly through the phase-interaction term, $-\gamma F_{12}$ and indirectly through the suppression of the production term, $\gamma^2\langle u_2' u_2'\rangle$, in the evolution equation of $-\gamma\langle u_1' u_2'\rangle$ (not shown here).

The energy production increases with gravity. The augmentation of turbulence at $V_S^+ = 2$ is caused by this increase of Reynolds shear stress. The phase-interaction

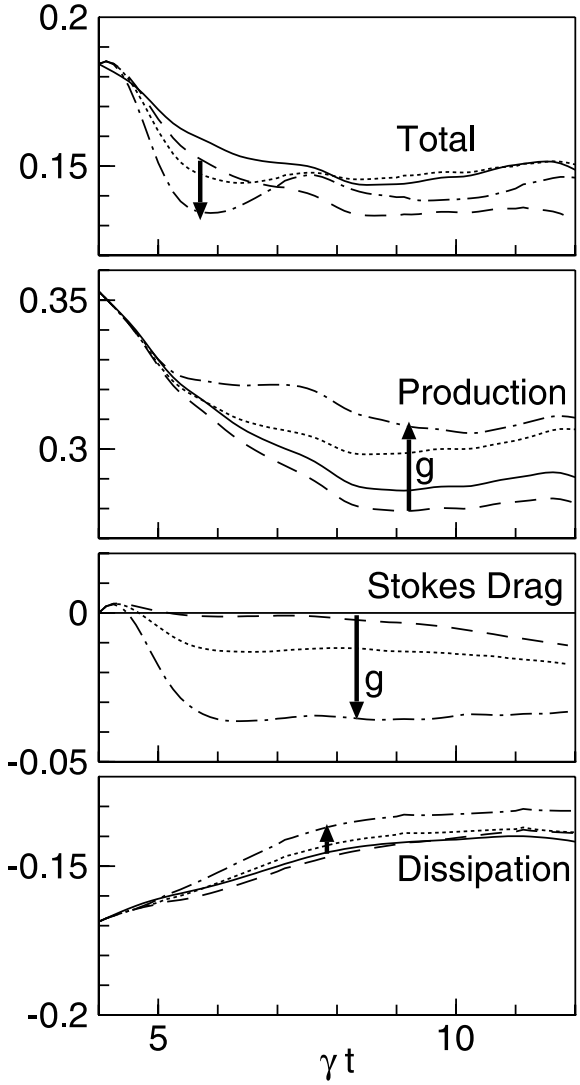

Fig. 3. Time development of the growth rate of the turbulence kinetic energy and contributions to the growth rate from the production, dissipation and phase-interaction terms: (—) single-phase, (- - -) $V_S^+ = 0$, (···) $V_S^+ = 2$, (–·–) $V_S^+ = 4$.

term, on the other hand, takes large negative values for $V_S^+ \gg 1$, which suppresses the development of turbulence, particularly in an initial period.

The phase-interaction term affects the fluid flow differently depending on the directions. Fig. 4 shows the time development of the phase-interaction term, F_{ii}, in the evolution equation of $\langle u_i' u_i'\rangle$. In the case of zero gravity, the streamwise component, F_{11}, takes positive values and is greater than the other two components, F_{22} and F_{33}. This is consistent with the previous finding (Reeks, 1993; Liljegren, 1993; Simonin et al., 1995) that the effect of the mean shear and the particle inertia increases the streamwise particle velocity variance. The vertical component, F_{22}, increases with gravity, which indicates that some of the potential energy of the particles in gravity is being converted to the kinetic energy

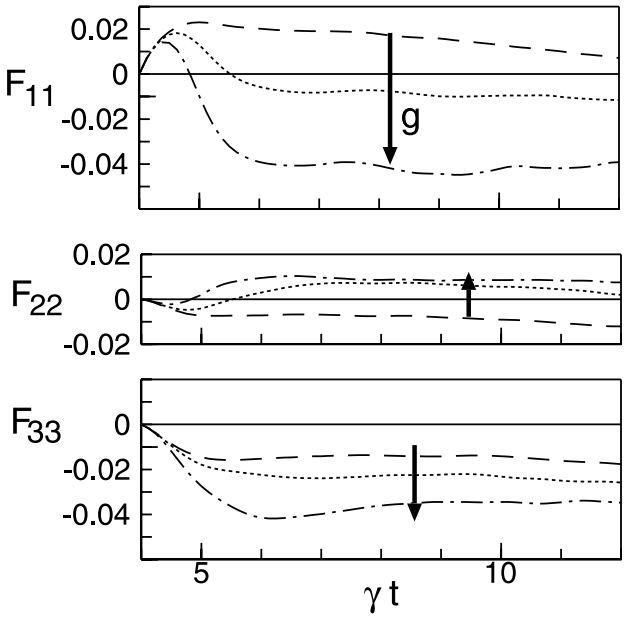

Fig. 4. Time development of F_{ii} (Eq. (7)): (—) single-phase, (- - -) $V_S^+ = 0$, (···) $V_S^+ = 2$, (–·–) $V_S^+ = 4$.

of the carrier fluid. The streamwise and spanwise components, on the other hand, decrease with the increase of gravity. Since the surrounding fluid velocity of a falling particle changes rapidly due to the crossing trajectories effect (Csanady, 1963), the particle turbulence kinetic energy is effectively reduced by its inertia. This may lead to the reduction of fluid kinetic energy as well through the two-way coupling between two phases. The noticeable decrease of F_{11} compared to that of F_{33} is caused by the interaction between particle clusters and vortical structures (see Section 3.3). The relations $F_{11} > 0$ and $F_{33} < F_{22} < 0$ in zero gravity were also found in Ahmed and Elghobashi (2000).

Finally, we briefly mention the dependence on the particle response time (figures are not shown). For $V_S^+ = 0$, the reduction rate of turbulence kinetic energy increases with τ_p, which is in agreement with the result in Ahmed and Elghobashi (2000). This is mainly caused by the increase in the drag dissipation. The augmentation of turbulence due to (small or moderate) gravity is more noticeable at smaller values of τ_p. This is because the particle inertia suppresses the increase of Reynolds shear stress due to gravity. The anisotropy of velocity and vorticity fields, on the other hand, exhibits relatively weak dependence on the particle inertia, and its change due to gravity is qualitatively the same for all of the three cases considered here.

3.2. Vorticity dynamics

The time development of turbulence enstrophy, $\langle \omega_k' \omega_k' \rangle$, is shown in Fig. 5. The presence of particles in zero gravity enhances the development of the enstrophy

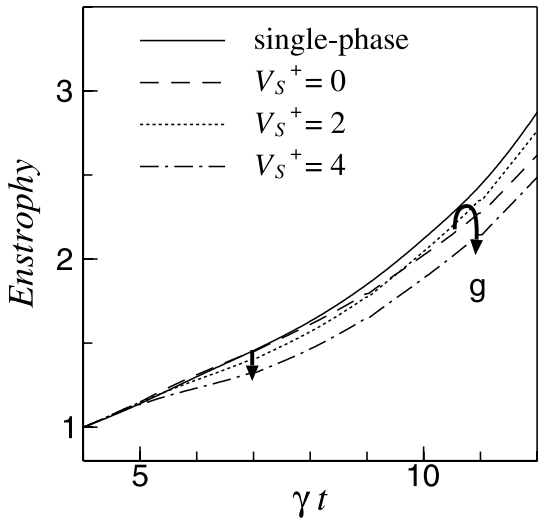

Fig. 5. Time development of turbulence enstrophy: (—) single-phase, (- - -) $V_S^+ = 0$, (···) $V_S^+ = 2$, (–·–) $V_S^+ = 4$.

slightly in the initial instant, but suppresses it significantly for $\gamma t > 7$. The enstrophy is reduced further for $V_S^+ = 4$.

The particles modulate the vorticity field in an anisotropic manner. Fig. 6 shows the time development of the anisotropy tensor of vorticity field, $w_{ij} = \langle \omega_i' \omega_j' \rangle /$

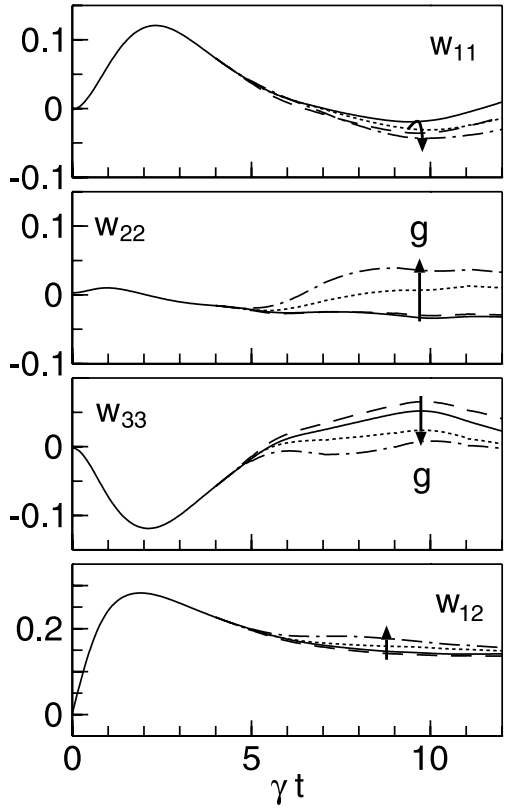

Fig. 6. Time development of vorticity anisotropy tensor: (—) single-phase, (- - -) $V_S^+ = 0$, (···) $V_S^+ = 2$, (–·–) $V_S^+ = 4$.

$\langle \omega'_k \omega'_k \rangle - (1/3)\delta_{ij}$. For times $\gamma t < 4$, w_{11} takes positive values, which corresponds to the development of quasi-streamwise vortex tubes. These vortices induce the strong straining flows, which stretch the mean shear vorticity to generate the vortex layers with negative spanwise vorticity. The increase of w_{33} after $\gamma t = 2$ corresponds to this development of the vortex layers (Kida and Tanaka, 1994). Decrease of w_{33} for $\gamma t > 10$ indicates that some of the vortex layers have rolled up into hairpin vortices. The presence of particles in zero gravity reduces the relative magnitude of streamwise vorticity w_{11}, and increases that of spanwise vorticity w_{33}. In finite gravity, the injection of particles leads to the increase in w_{22} and w_{12}, and to the decrease in w_{33}.

In order to gain further insight into the modification of the vorticity field, we introduce the orientation angles α and β of vorticity vector, which are defined as (Kawahara et al., 1997)

$$\begin{aligned} \omega_1 &= |\boldsymbol{\omega}| \cos\alpha, \\ \omega_2 &= |\boldsymbol{\omega}| \sin\alpha \cos\beta, \\ \omega_3 &= |\boldsymbol{\omega}| \sin\alpha \sin\beta, \end{aligned} \tag{11}$$

where $\omega_i = \omega'_i - \gamma\delta_{i3}$ is the total vorticity (Fig. 7). Fig. 8 shows the probability density function (pdf) of orientation angles α and β of the vorticity weighted by $\boldsymbol{\omega}^2$, that is, the directional distribution of the local enstrophy. For the single-phase flow, the pdf was normalized such that the integral of the pdf over all orientation has the value of unity. In order to observe the change of vorticity amplitude due to the two-way coupling effects, the pdfs for the other cases were also normalized by the same normalization factor as that used for the single-phase flow. The contour lines of level 1 is represented by the bold line. The peak in the center ($\alpha = \pi/2$, $\beta = -\pi/2$) of each figure corresponds to the vortex layers with negative spanwise vorticity. The other two peaks located at ($\alpha \approx \pi/8$, $\beta = 0$) and ($\alpha \approx 7\pi/8$, $\beta = -\pi$) correspond to the quasi-streamwise vortices, which are inclined toward the x_2 direction from the x_1 direction.

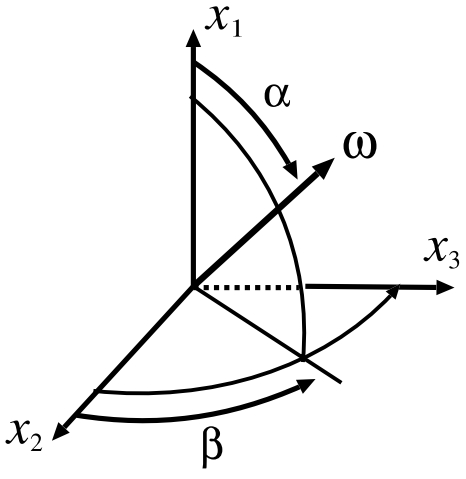

Fig. 7. Orientation angles α and β.

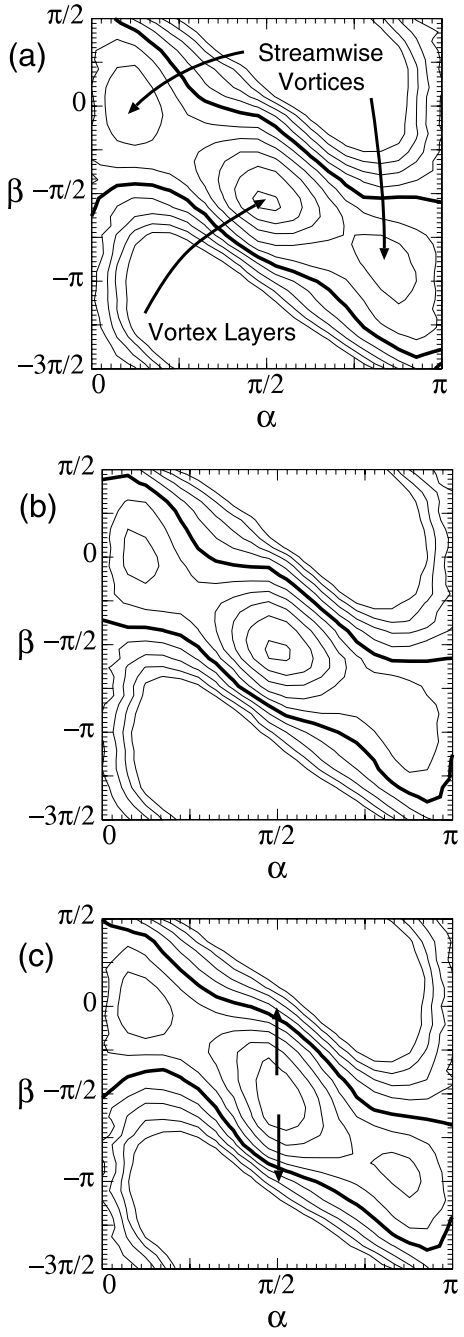

Fig. 8. Directional distribution of enstrophy at $\gamma t = 12$ for (a) single-phase flow, (b) $V_S^+ = 0$ and (c) $V_S^+ = 2$. Contour levels are 2^p ($p = -4, -3.5, -3, \ldots$). The bold line represents the contour line of level 1.

Comparing Fig. 8(a) and (b), we notice that the peak values of the pdf corresponding to the quasi-streamwise vortices become smaller by the presence of particles in zero gravity, indicating the attenuation of the quasi-streamwise vortices. This is in agreement with the

analytical results in Druzhinin (1995a,b), which show that the vorticity is reduced at the cores of vortex tubes, due to the effect of two-way coupling. The peak corresponding to the vortex layers, on the other hand, takes a slightly larger value than that in the single-phase flow (it is more noticeable at earlier times when the attenuation of turbulence is less significant). This indicates the existence of a mechanism that leads to the intensification of the vortex layers. For $V_S^+ = 2$, the streamwise vortices are intensified compared to the case of $V_S^+ = 0$. Another distinguished feature in finite gravity is the modification of the enstrophy distribution around the peak corresponding to the vortex layers (Fig. 8(c)). The distribution is elongated in the $\pm x_2$ direction ($\alpha = \pi/2$, $\beta = 0$, $-\pi$) as is denoted by arrows. It is interesting to note that the drag forces do not directly generate the vertical vorticity component if they are pointed to the gravitational direction. Further analysis of the evolution equation of vorticity has clarified that the vertical vorticity is mainly generated by the non-linear (stretching-and-tilting) term in the equation. In the next subsection, we will show that the generation of the vertical vorticity is caused by the tilting of vortex layers due to particle clusters (Fig. 10).

3.3. Interaction between vortical structures and particle clusters

In Fig. 9, we plot the averaged value of the particle concentration conditioned on the spanwise vorticity, ω_3'.

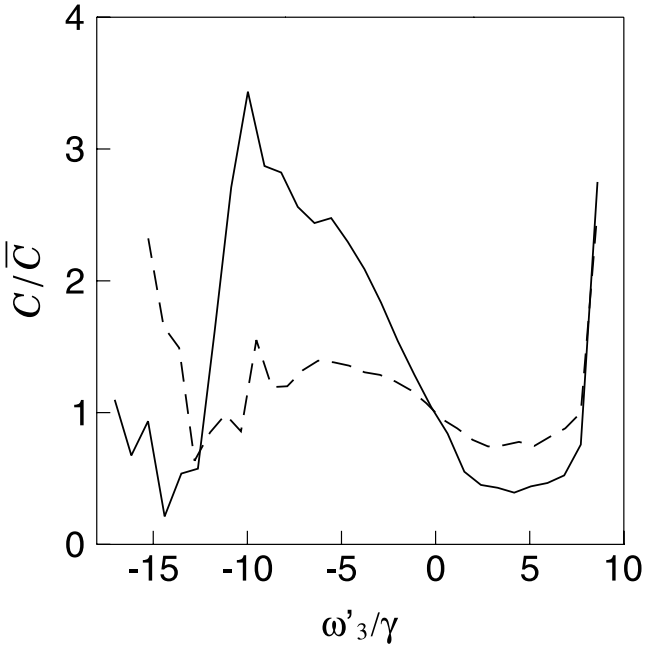

Fig. 9. Particle concentration as a function of the spanwise vorticity, ω_3', at $\gamma t = 12$. (—) $V_S^+ = 0$, (- - -) $V_S^+ = 2$.

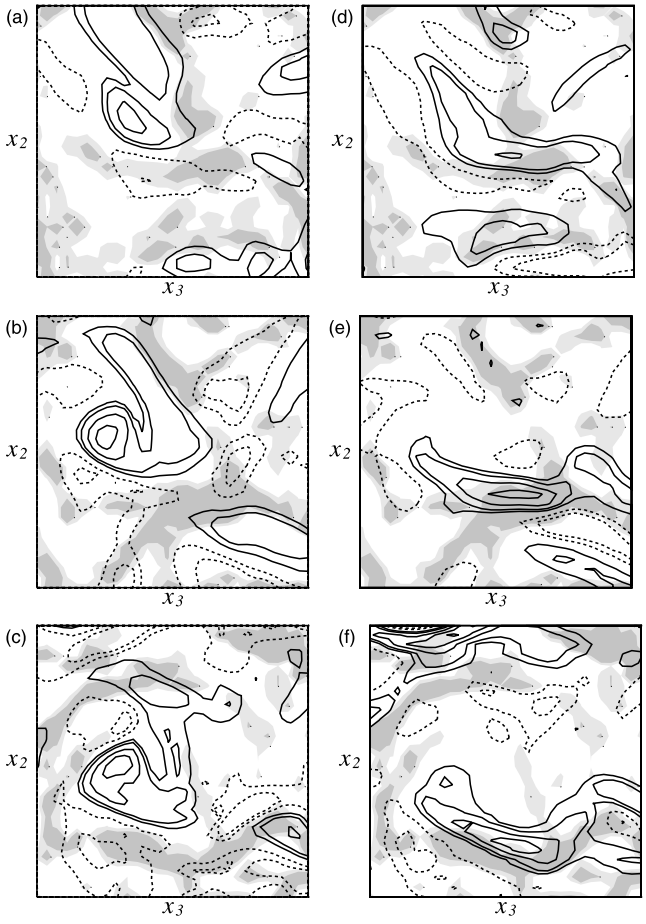

Fig. 10. Typical example of the interactions between particle clusters and vortical structures for $V_S^+ = 2$. (a, d) $\gamma t = 10$, (b, e) $\gamma t = 11$, (c, f) $\gamma t = 12$. Spatial distributions of (a)–(c) streamwise and (d)–(f) spanwise components of vorticity and local concentration of particles are shown in a region of $28(2\pi/128) \times 28(2\pi/128)$ in the x_3–x_2 planes. Darker and lighter shades denote the regions of $C \geqslant 2\overline{C}$ and $C \geqslant \overline{C}$, respectively. Contour lines of $\omega_1' = \gamma$, 2γ, 4γ, 6γ ($-\gamma$, -2γ, -4γ, -6γ) are denoted by solid (broken) lines in (a)–(c), while those of $\omega_3' = -\gamma$, -2γ, -4γ, -6γ (γ, 2γ, 4γ, 6γ) are represented by solid (broken) lines in (d)–(f).

The tendency of particles to concentrate in the regions of large negative values of spanwise vorticity is clearly seen in zero gravity, which indicates that the particle clustering is taking place at the vortex layers with negative spanwise vorticity. In finite gravity, the distribution is flattened. In fact, the particles tend to accumulate beneath the vortex layers due to gravity (see Fig. 10(f)).

Now, let us examine the interactions of particle clusters with vortical structures in order to identify the processes that control the aforementioned phenomena. Fig. 10 shows a typical example of such interaction observed in the case of $V_S^+ = 2$. Fig. 10(a)–(c) and (d)–(e) respectively show the spatial distributions of streamwise and spanwise vorticities on the x_3–x_2 planes. Solid (broken) lines in Fig. 10(a)–(c) represent quasi-

streamwise vortices which induce flows rotating clockwisely (counter clockwisely), while solid lines in Fig. 10(d)–(e) represent vortex layers with negative spanwise vorticity. Shaded regions in each figure indicate high-concentrated regions of the particles. The darker and lighter shades denote the regions of $C \geqslant 2\overline{C}$ and $C \geqslant \overline{C}$, respectively, where C denotes the local volume fraction of particles. Note that the cross section is moving in the x_1 direction with the structures from $\gamma t = 10$ (Fig. 10(a) and (d)) to $\gamma t = 12$ (Fig. 10(c) and (f)). Here, we focus on three pairs of counter rotating quasi-streamwise vortices seen in Fig. 10(b). These vortex pairs are labeled by A, B1 and B2 and marked by bold lines in Fig. 11(a). The arrow indicates the direction of the flow induced by the vortex pair. As is illustrated in Fig. 11(b), two vortex pairs, aligned in the x_3 direction, induce a strong straining flow between them, which stretches the mean spanwise vorticity, as indicated by arrows, to generate the vortex layer (Kida and Tanaka, 1994). A strong vortex layer of negative spanwise vorticity seen in Fig. 10(d)–(f) is being stretched by the two vortex pairs, B1 and B2.

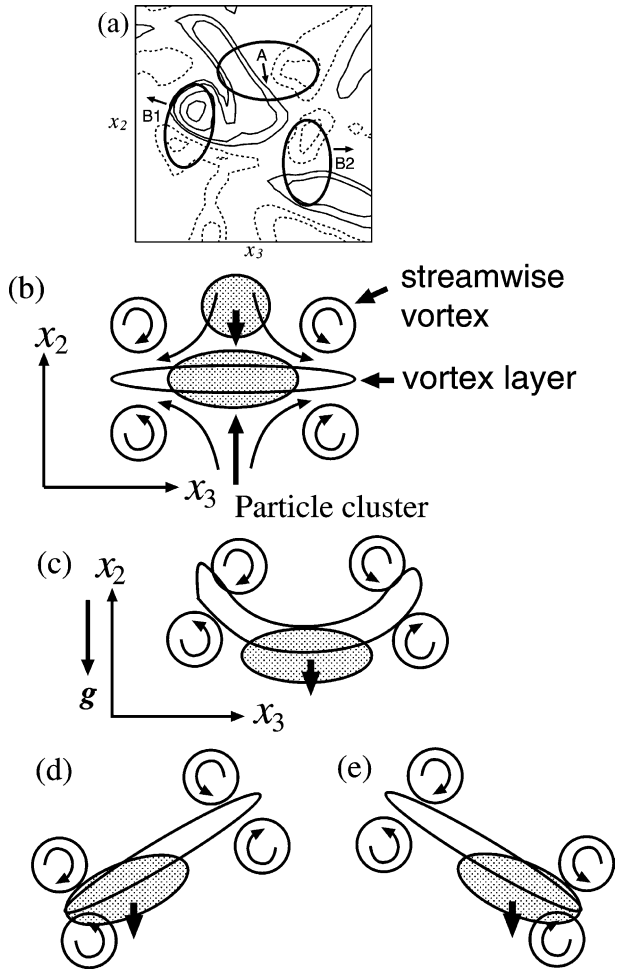

Fig. 11. Skematic of the interaction between a particle cluster and vortical structures. Thin contour lines in (a) are the same as those in Fig. 10(b), while thick lines in the figure denote the counter rotating vortex pairs.

The settling particles are found to accumulate typically in two types of regions. We notice that the particles are concentrated into the downward fluid between the pair vortices A as in the case of isotropic turbulence (Wang and Maxey, 1993). Another type of particle cluster, which is rather horizontal, is found along the vortex layer. Since the development of vortex layers is often accompanied by high strain induced by vortex pairs, small heavy particles tend to accumulate in the vortex layers (see Fig. 11(b)). Because of the gravity, the particles approach the vortex layer from above and a particle cluster is eventually generated just beneath the layer. Due to the downward flow induced by the cluster, the vortex layer (and negative spanwise vorticity vectors therein) is tilted toward the vertical direction as is shown in Fig. 10(f). The vortex layer is deformed to a concave shape by the induced flow as shown in Fig. 11(c) if the symmetry of the structures in the spanwise direction is sufficiently high. In general, the difference in strength of the four quasi-streamwise vortices causes asymmetry, and thus in most cases the vortex layer is tilted by the cluster as shown in Fig. 11(d) or (e).

These vortex structures and particle clusters play an important role in the evolution of turbulence energy. In Fig. 12(a), regions of high Reynolds shear stress, $-\gamma\langle u_1' u_2' \rangle \geqslant 0.05$, are represented by light shades for the single-phase flow on the same plane as Fig. 10(b) and (e). Bold solid line represents the vortex layer of negative spanwise vorticity. It is seen that the Reynolds shear stress takes large values in the area between the pair vortices A (Kida and Tanaka, 1992). The presence of particles in zero gravity attenuates the Reynolds shear stress (not shown) because the vortex pair A is weakened by the particles. In the case of $V_S^+ = 2$ to the contrary, it is enhanced in the region A as is shown in Fig. 12(b). These results are consistent with those of Ahmed and Elghobashi (2000). The enhancement of the Reynolds shear stress in finite gravity is found to be caused by the successive passing of particle clusters, which has intensified the flow between the pair vortices in the negative x_2 and positive x_1 directions. In Fig. 12(c), dark shades denote the regions of large negative values of the direct energy transfer due to the particles (F in Eq. (7)). It is seen that the transfer takes large negative values in the area beneath the vortex layer. It is found that this negative transfer mainly comes from the streamwise component, F_{11} (not shown).

Fig. 13 illustrates the mechanism of the negative energy transfer that occurs when a cluster passes across a vortex layer as a result of gravitational settling. In the vortex layer, the streamwise component of the fluid velocity decreases sharply in the gravitational (negative x_2)

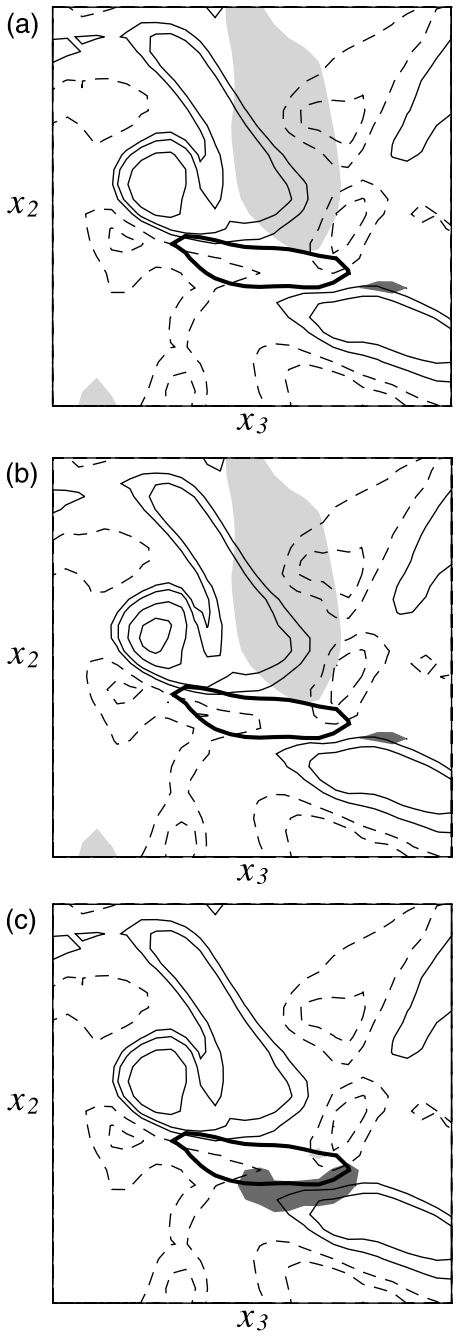

Fig. 12. The spatial distribution of Reynolds shear stress, $-\gamma u_1 u_2$, at $\gamma t = 11$ is plotted on the same plane as Fig. 10(b) for (a) the single-phase flow and (b) $V_S^+ = 2$. Light and dark shades denote the regions of $-\gamma u_1 u_2 \geqslant 0.05$ and $-\gamma u_1 u_2 \leqslant -0.05$, respectively. (c) The same as Fig. 12(b) except that light and dark shades denote the regions of $F \geqslant 0.05$ and $F \leqslant 0.05$, respectively. Contour lines of $\omega_1' = \gamma$, 2γ, 4γ, 6γ ($-\gamma$, -2γ, -4γ, -6γ) are represented by thin solid (broken) lines. Bold solid line represents the regions of $\omega_3' \leqslant -3\gamma$.

direction. Because of their inertia, the settling particles cannot follow the sharp decrease of the streamwise fluid velocity and thus slip (relative to the surrounding fluid)

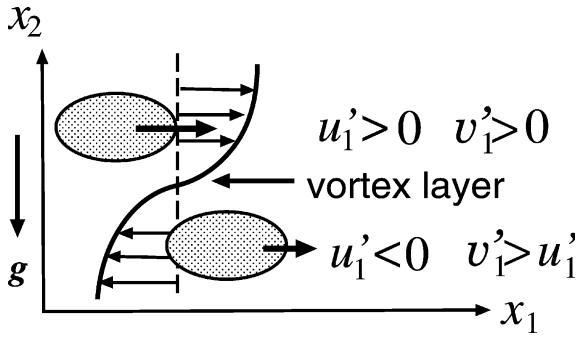

Fig. 13. Drag dissipation due to the particle cluster.

in the positive streamwise direction (see Eq. (6)). Since, in general, the streamwise component of fluctuating fluid velocity is negative beneath the vortex layer, the drag forces in the positive streamwise direction reduce the streamwise fluid velocity variance.

4. Conclusions

Numerical simulations have been carried out for a homogeneous turbulent shear flow laden with small heavy particles in the so-called two-way coupling regime, where the effects of inter-particle collisions are negligible, but the effects of the particulate phase on the fluid phase should be considered. We have investigated the particle clustering and the resulting turbulence modification, focusing attentions on the interaction of the particle clusters with the vortical structures in the turbulence. The particles whose response times are comparable to the Kolmogorov time-scale of the turbulence are considered, taking account of the previous finding that the preferential concentration of particles (or particle clustering) is most noticeable for these particles. The effects on the turbulence modification of the gravity in the sheared direction have been examined to obtain the following results:

(1) In the case of zero gravity and moderate particle inertia, the presence of particles suppresses the development of turbulence kinetic energy of the carrier fluid. At a finite value of gravity ($V_S^+ = 2$), the particles enhances the development of the turbulence energy by the intensification of Reynolds shear stress. At a larger value of gravity ($V_S^+ = 4$), however, the fluid turbulence is attenuated by the direct phase-interaction with the particles.
(2) The particles in finite gravity tend to accumulate in the two types of regions; downward flows sandwiched between counter rotating quasi-streamwise vortex tubes and regions beneath the vortex layers with negative spanwise vorticity.

(3) The particle clusters between the pair vortex tubes intensify the downward flows between them to enhance the Reynolds shear stress.
(4) The particle clusters beneath the vortex layers enhances the drag dissipation of the fluid turbulence energy in the streamwise direction.
(5) The particle clusters induce the downward flows, which tilt the spanwise vorticity in the vortex layers to the vertical direction. This results in the increase of the relative magnitude of the vertical vorticity.

Our numerical results indicate that the interaction between the particle clusters and the vortical structures plays an essential role in the turbulence modification when the particle response time is of the order of the Kolmogorov time-scale. It is also shown that the interaction is considerably affected by the gravity for the particle settling velocity comparable to the Kolmogorov velocity. Though no relevant experiments have been conducted so far, the gravity is expected to be important in some practical situations (see Appendix A).

Results obtained in this study show that the particle clusters under gravity affect the growth of fluid turbulence energy directly by the enhancement of Reynolds shear stress and drag dissipation. They also influence the growth of energy indirectly by modifying the dynamics of the vortical structures in the sheared turbulence. Relative importance of the indirect effects may increase at higher Reynolds numbers. Therefore, it is important to understand how every stage of the vortex dynamics, i.e., the generation, development and interaction of vortical structures, is affected by the particles. Further details of the vortex dynamics, such as the regeneration of quasi-streamwise vortices through roll-ups of the vortex layers, should be examined in future studies.

Appendix A. On the effect of gravity

Our simulation indicates the importance of the gravity for the turbulence dynamics. Unfortunately, no available experimental data have been obtained so far in the parameter range where our simulation was conducted. However, practical values of normalized gravity, $g^+ = g\tau_K^2/\eta$, can be estimated for previous experiments of (single-phase) homogeneous turbulent shear flows as $g^+ \approx 2.0$ for Champagne et al. (1970), 0.3 for Tavoularis and Corrsin (1981), and 0.1–1.0 for Tavoularis and Karnik (1989). By comparing our numerical results of $\tau_p^+ = 2$, $V_S^+ = 1$ with those of $\tau_p^+ = 2$, $V_S^+ = 0$, we have found that the effects of the gravity of $g^+ \approx 0.5$ are comparable to those the particles in zero gravity have on the single-phase flow. Therefore, the effect of gravity may be important for the experiments of particle-laden flows which would be conducted under the flow conditions employed in the previous experiments.

References

Ahmed, A.M., Elghobashi, S., 2000. On the mechanisms of modifying the structure of turbulent homogeneous shear flows by dispersed particles. Phys. Fluids 12 (11), 2906–2930.

Aliseda, A., Cartellier, A., Hainaux, F., Lasheras, J.C., 2002. Effect of preferential concentration on the settling velocity of heavy particles in homogenous isotropic turbulence. J. Fluid Mech., to appear.

Champagne, F.H., Harris, V.G., Corrsin, S., 1970. Experiments on nearly homogeneous turbulent shear flow. J. Fluid Mech. 41, 81–139.

Csanady, G.T., 1963. Turbulent diffusion of heavy particles in the atmosphere. J. Atmos. Sci. 20, 201–208.

Druzhinin, O.A., 1995a. On the two-way interaction in two-dimensional particle-laden flows: the accumulation of particles and flow modification. J. Fluid Mech. 297, 49–76.

Druzhinin, O.A., 1995b. The dynamics of a concentration interface in a dilute suspension of solid heavy particles. Phys. Fluids 7 (9), 2132–2142.

Elghobashi, S., Truesdell, G.C., 1993. On the two-way interaction between homogeneous turbulence and dispersed solid particles. I. Turbulence modification. Phys. Fluids A 5 (7), 1790–1801.

Kawahara, G., Kida, S., Tanaka, M., Yanase, S., 1997. Wrap, tilt and stretch of vorticity lines around a strong thin straight vortex tube in a simple shear flow. J. Fluid Mech. 353, 115–162.

Kida, S., Tanaka, M., 1992. Reynolds stress and vortical structure in a uniformly sheared turbulence. J. Phys. Soc. Japan 61 (12), 4400–4417.

Kida, S., Tanaka, M., 1994. Dynamics of vortical structures in a homogeneous shear flow. J. Fluid Mech. 274, 43–68.

Kulick, J.D., Fessler, J.R, Eaton, J.K., 1994. Particle response and turbulence modification in fully developed channel flow. J. Fluid Mech. 277, 109–134.

Liljegren, L.M., 1993. The effect of a mean fluid velocity gradient on the streamwise velocity variance of a particle suspended in a turbulent flow. Int. J. Multiphase Flow 19 (3), 471–484.

Mashayek, F., 1998. Droplet–turbulence interactions in low-Mach-number homogeneous shear two-phase flows. J. Fluid Mech. 367, 163–203.

Maxey, M.R., Riley, J.J., 1983. Equation of motion for a small rigid sphere in a nonuniform flow. Phys. Fluids 26 (4), 883–889.

Reeks, M.W., 1993. On the constitutive relations for dispersed particles in nonuniform flows. I. Dispersion in a simple shear flow. Phys. Fluids A 5 (3), 750–761.

Rogers, C.B., Eaton, J.K., 1991. The effect of small particles on fluid turbulence in a flat-plate, turbulent boundary layer in air. Phys. Fluids A 3 (5), 928–937.

Simonin, O., Deutsch, E., Boivin, M., 1995. Large eddy simulation and second-moment closure model of particle fluctuating motion in two-phase turbulent shear flows. In: Durst, F. et al. (Eds.), Turbulent Shear Flows, vol. 9. Springer, Berlin.

Squires, K.D., Eaton, J.K., 1990. Particle response and turbulence modification in isotropic turbulence. Phys. Fluids A 2 (7), 1191–1203.

Squires, K.D., Eaton, J.K., 1991. Preferential concentration of particles by turbulence. Phys. Fluids A 3 (5), 1169–1178.

Sundaram, S., Collins, L.R., 1996. Numerical considerations in simulating a turbulent suspension of finite-volume particles. J. Comput. Phys. 124 (2), 337–350.

Tanaka, M., Komai, N., Maeda, Y., Hagiwara, Y., 2000. Two-way coupling effect on settling velocity of small heavy particles in

homogeneous turbulence. In: Dopazo, C. et al. (Eds.), Advances in Turbulence VIII. CIMNE, Barcelona.

Tavoularis, S., Corrsin, S., 1981. Experiments in nearly homogeneous turbulent shear flow with a uniform mean temperature gradient, part I. J. Fluid Mech. 104, 311–347.

Tavoularis, S., Karnik, U., 1989. Further experiments on the evolution of turbulent stresses and scales in uniformly sheared turbulence. J. Fluid Mech. 204, 457–478.

Tsuji, Y., Morikawa, Y., 1982. LDV Measurements of an air–solid two-phase flow in a horizontal pipe. J. Fluid Mech. 120, 385–409.

Tsuji, Y., Morikawa, Y., Shiomi, H., 1984. LDV Measurements of an air–solid two-phase flow in a vertical pipe. J. Fluid Mech. 139, 417–434.

Wang, L.P., Maxey, M.R., 1993. Settling velocity and concentration distribution of heavy particles in homogeneous isotropic turbulence. J. Fluid Mech. 256, 27–68.

Yamamoto, Y., Potthoff, M., Tanaka, T., Kajishima, T., Tsuji, Y., 2001. Large-eddy simulation of turbulent gas-particle flow in a vertical channel: effect of considering inter-particle collisions. J. Fluid Mech. 442, 303–334.